Low-energy physical properties of high-T_c superconducting Cu oxides: A comparison between the resonating valence bond and experiments

Kai-Yu Yang,[1] C. T. Shih,[2] C. P. Chou,[3] S. M. Huang,[3] T. K. Lee,[3] T. Xiang,[4] and F. C. Zhang[1,5]
[1]*Centre of Theoretical and Computational Physics and Department of Physics, The University of Hong Kong, Hong Kong*
[2]*Department of Physics, Tunghai University, Taichung, Taiwan*
[3]*Institute of Physics, Academia Sinica, Taipei, Taiwan*
[4]*Institute of Theoretical Physics and Interdisciplinary Center of Theoretical Studies, Chinese Academy of Sciences, Beijing, China*
[5]*Department of Physics, University of Cincinnati, Cincinnati, Ohio 45221, USA*
(Received 16 March 2006; published 16 June 2006)

In a recent review by Anderson and co-workers, it was pointed out that an early resonating valence bond (RVB) theory is able to explain a number of unusual properties of high-temperature superconducting (SC) Cu oxides. Here we extend previous calculations to study more systematically the low-energy physical properties of the plain vanilla *d*-wave RVB state, and to compare the results with the available experiments. We use a renormalized mean-field theory combined with variational Monte Carlo and power Lanczos methods to study the RVB state of an extended *t-J* model in a square lattice with parameters suitable for the hole-doped Cu oxides. The physical observable quantities we study include the specific heat, the linear residual thermal conductivity, the in-plane magnetic penetration depth, the quasiparticle energy at the antinode $(\pi,0)$, the superconducting energy gap, the quasiparticle spectra, and the Drude weights. The traits of nodes (including k_F, the Fermi velocity v_F, and the velocity along Fermi surface v_2), and the SC order parameter are studied. Comparisons of the theory and the experiments in cuprates show an overall qualitative agreement, especially on their doping dependences.

DOI: 10.1103/PhysRevB.73.224513 PACS number(s): 74.20.Fg, 74.72.−h, 71.10.−w

I. INTRODUCTION

Since the discovery of high transition temperature superconductivity (HTSC) in cuprates in 1986, there have been enormous efforts in both experiments and theories to understand the mechanism of the superconductivity and their unusual physical properties. One of the earliest theory is the resonating valence bond (RVB) theory proposed by Anderson.[1] In that theory, the operative element in the electronic structure of this class of compounds is the square planar CuO_2 lattice. The parent compound such as La_2CuO_4, where the Cu is stoichiometrically bivalent Cu^{2+} with one hole per Cu site, is an antiferromagnetically coupled Mott insulator. Chemical doping such as the partial replacement of La by Sr introduces additional holes on the CuO_2 planes. The minimum microscopic model to describe the low-energy physics has been proposed to be the *t-J* model or its variant extended *t-J* model, which includes an antiferromagnetic spin coupling and a kinetic energy term for the hole motion.[1,2] Anderson proposed a doped spin liquid of spin singlets, or the bond spin singlet resonating between many configurations.[1] This concept explains many unusual properties of the cuprates, as emphasized in a recent review by Anderson and co-workers.[3] More quantitatively, in the simplest RVB theory, namely its plain vanilla version, the RVB state in the cuprate is described by a Gutzwiller projected *d*-wave BCS wave function, whose parameters are determined variationally either by using a renormalized mean field theory[4] (RMFT) or by variational Monte Carlo method (VMC) numerically,[5–7] or by other field theory methods.[8] Recently the Gutzwiller RVB wave function approach was applied to the strong coupling Hubbard model by Paramekanti, Randeria, and Trivedi, who used careful numerical methods to calculate several quantities of direct experimental relevance.[9] Both results for the Hubbard and *t-J* models turn out to correspond well to some experimental phenomena observed in cuprates. The plain vanilla RVB theory has recently been extended to study the scanning tunneling microscopy, the angle resolved photoemission spectroscopy[10] (ARPES) and the Gossamer superconductivity[11] in the Hubbard-like models at the half electron filling. In view of the preliminary success of the plain vanilla RVB theory, it is desirable to extend previous calculations and to analyze more experimental data so that a more systematic and comprehensive comparison between the theories[12,13] and the experiments[14] can be made on more observable quantities.

In the present paper, we extend the previous works of Zhang *et al.*[4] and of Paramekanti *et al.*[9] to carry out more systematic calculations on the low-energy physical properties of the plain vanilla *d*-wave RVB state. We use a renormalized mean-field theory combined with variational Monte Carlo and power Lanczos (PL) methods[15,16] to study the RVB state of an extended *t-J* model in a square lattice for parameters suitable for the hole doped lanthanum and yttrium Cu oxides. Our main focus is on the microscopic calculations of the key parameters for nodal quasiparticles in the *d*-wave RVB state, namely, the Fermi velocity v_F and the velocity along the Fermi surface v_2. From these quantities, we calculate a number of low-energy physical properties including the specific heat, the linear residual thermal conductivity, and the in-plane magnetic penetration depth. We make extensive comparison between these calculations with a very broad spectrum of types of reported experiments, and find qualitative agreement, especially on the doping dependences of these properties. The discrepancy between the theory and experiments is mostly on the absolute values of these quan-

TABLE I. Parameters $\{t,t'/t,t''/t,J/t\}$ for $La_{2-x}Sr_xCuO_4$ and $YBa_2Cu_3O_{7-x}$ ($Bi_2Sr_2CaCu_2O_{8+x}$) used in the renormalized mean field theory.

	t(eV)	t'/t	t''/t	J/t
$La_{2-x}Sr_xCuO_4$	0.3	−0.1	0.05	0.3
$YBa_2Cu_3O_{7-x}$	0.3	−0.3	0.2	0.3
$Bi_2Sr_2CaCu_2O_{8+x}$				

tities, which may be attributed to a factor of 2–4 times larger in the value of v_2 in the theory. We also calculate the quasiparticle energy gap at the antinode $(\pi,0)$, the superconducting (SC) energy gap, the quasiparticle spectra, and the Drude weight. We find good agreements with experiments.

The paper is organized as follows. In Sec. II, we describe the microscopic model and the methods we used in our calculations. In Sec. III, we calculate the basic parameters of the nodal quasiparticles. In Sec. IV, we discuss the nodal physics and make comparison of the theory and experiments on a number of low energy physical properties. In Sec. V, we calculate other physical quantities and compare with the experiments. A brief summary is given in Sec. VI.

II. MODEL AND METHODS

A. Model

We consider an extended *t-J* model including a nearest-neighbor (NN), a second NN and a third NN hopping terms in the square lattice,

$$H = H_t + H_J,$$

$$H_t = -t\sum_{\langle i,j\rangle,\sigma} c^\dagger_{i\sigma}c_{j\sigma} - t'\sum_{\langle i,j\rangle',\sigma} c^\dagger_{i\sigma}c_{j\sigma} - t''\sum_{\langle i,j\rangle'',\sigma} c^\dagger_{i\sigma}c_{j\sigma},$$

$$H_J = J\sum_{\langle i,j\rangle} \mathbf{S}_i\cdot\mathbf{S}_j. \tag{1}$$

In the above Hamiltonian, a constraint of no double occupation of electrons on any site is implied: $\Sigma_\sigma c^\dagger_{i,\sigma}c_{i,\sigma}\leqslant 1$. The summations $\langle i,j\rangle, \langle i,j\rangle'$, and $\langle i,j\rangle''$ run over the NN, second NN, and third NN pairs. t, t' and t'' are their corresponding hopping integrals, respectively. We choose t, t'' to be positive, and t' to be negative, appropriate for the hole-doped cuprates, J is the superexchange coupling between the NN spins. Table I lists the parameters $\{t,t'/t,t''/t,J/t\}$ used in our calculations for monolayered $La_{2-x}Sr_xCuO_4$ (LSCO) and bilayered cuprate $YBa_2Cu_3O_{7-x}$ (YBCO) or $Bi_2Sr_2CaCu_2O_{8+x}$ (Bi-2212). These parameters appear consistent with the band structure calculations[17] and also with the experimental analyses such as the topology of large Fermi surface reported in ARPES,[18,19] the inelastic light scattering,[20] neutron scattering,[21–23] and two-magnon Raman scattering experiments.[24–26]

We use a variational projected *d*-wave BCS state or the *d*-RVB state to study the ground state and elementary excitations of the model.[1] The trial ground state is of the form

$$|\Psi_L\rangle = P_G|\Psi_{\rm BCS}\rangle, \tag{2}$$

where the Gutzwiller projection operator $P_G=\Pi_i(1-n_{i\uparrow}n_{i\downarrow})$ is to ensure the constraint of no double occupation of electrons on any lattice site. The BCS state is of the standard form, given by

$$|\Psi_{\rm BCS}\rangle = \prod_{\mathbf{k}} (u_{\mathbf{k}} + v_{\mathbf{k}}c^\dagger_{\mathbf{k}\uparrow}c^\dagger_{-\mathbf{k}\downarrow})|0\rangle,$$

where $|0\rangle$ is the vacuum state, and $u_{\mathbf{k}}$ and $v_{\mathbf{k}}$ are the variational parameters satisfying the normalization condition: $|u_{\mathbf{k}}|^2+|v_{\mathbf{k}}|^2=1$.

In this paper, we use two complementary methods to carry out the Gutzwiller projected variational calculation. One is the renormalized mean field theory, which takes into account of the Gutzwiller projection by a set of renormalization factors.[4] The other is the variational Monte Carlo method which computes the quantities numerically, followed by a further improvement of the variational wave function by using the PL method to eliminate or to reduce the bias in the variational approach.[15,16] It is well known that the variational calculation often over-estimates the effect of superconductivity in the true ground state, and the variational calculation usually leads to a larger Δ.[7]

B. Renormalized mean field theory

The RMFT is a Hartree-Fock-like mean-field theory to approximately treat the projection operator in the Hamiltonian in Eq. (1). In the RMFT, we apply the Gutzwiller approximation to replace the effect of the projection operator by a set of renormalization factors, which are determined by statistical counting.[4,27] The variation of a projected state for Hamiltonian H is then approximately mapped onto that of the corresponding unprojected state for a renormalized Hamiltonian.[3,4] This method was initially developed by Gutzwiller to study possible ferromagnetism in strongly interacting systems.[27] It was later applied by Brinkman and Rice to study the metal insulator transition, and by Vollhardt to study the Fermi liquid theory of helium-3.[28,29]

Let $\langle Q\rangle$ be an expectation value of Q in the RVB state $|\Psi_L\rangle$, and $\langle Q\rangle_0$ be an expectation value of Q in the BCS state $|\Psi_{\rm BCS}\rangle$, then the expectation values of the hopping term and the spin-spin correlation in the RVB states can be written in terms of those in the BCS state

$$\langle c^\dagger_{i\sigma}c_{j\sigma}\rangle = g_t\langle c^\dagger_{i\sigma}c_{j\sigma}\rangle_0,$$

$$\langle \mathbf{S}_i\cdot\mathbf{S}_j\rangle = g_s\langle \mathbf{S}_i\cdot\mathbf{S}_j\rangle_0. \tag{3}$$

g_t and g_s are the two renormalization factors for the kinetic and the spin-spin superexchange terms, respectively, they are given by

$$g_t = \frac{2\delta}{1+\delta}, \quad g_s = \frac{4}{(1+\delta)^2},$$

with δ the hole concentration.[4] The evaluation of H in the RVB state is then mapped onto the evaluation of the renormalized Hamiltonian H' in the corresponding BCS state, with H' given by

$$H' = g_t H_t + g_s H_J. \tag{4}$$

The variational energy of the system is then given by

$$W = \langle H \rangle = \langle H' \rangle_0.$$

In this paper, we shall only consider even parity SC state, namely, $|v_{-\mathbf{k}}|^2 = |v_{\mathbf{k}}|^2$ and $v_{\mathbf{k}}^* u_{\mathbf{k}} = u_{-\mathbf{k}}^* v_{-\mathbf{k}}$. We obtain

$$W = 2g_t \sum_{\mathbf{k}} |v_{\mathbf{k}}|^2 \varepsilon(\mathbf{k}) + \frac{g_s}{N} \sum_{\mathbf{k},\mathbf{k}'} V_{\mathbf{k}-\mathbf{k}'} (|v_{\mathbf{k}}|^2 |v_{\mathbf{k}'}|^2 + u_{\mathbf{k}} v_{\mathbf{k}} v_{\mathbf{k}'}^* u_{\mathbf{k}'}^*),$$

where

$$\varepsilon(\mathbf{k}) = -2t(\cos k_x + \cos k_y) - 4t'(\cos k_x \cos k_y) - 2t''(\cos 2k_x + \cos 2k_y),$$

$$V_{\mathbf{k}-\mathbf{k}'} = -\frac{3}{2} J[\cos(k_x - k_x') + \cos(k_y - k_y')],$$

with N the total number of lattice sites. The total number of electrons operator $N_e = \Sigma_{\mathbf{k}\sigma} c_{\mathbf{k}\sigma}^\dagger c_{\mathbf{k}\sigma}$ has an expectation value of $\langle N_e \rangle = 2\Sigma_{\mathbf{k}} |v_{\mathbf{k}}|^2$, so that the hole concentration

$$\delta = 1 - 2\sum_{\mathbf{k}} |v_{\mathbf{k}}|^2 / N. \tag{5}$$

Let μ be the chemical potential, the quantity we wish to minimize is $W' = \langle H - \mu N_e \rangle$, or

$$W' = W - 2\mu \sum_{\mathbf{k}} |v_{\mathbf{k}}|^2.$$

The variation is carried out with respect to $v_{\mathbf{k}}$, $u_{\mathbf{k}}$, and δ for fixed μ. Carrying out this variational procedure, we find that

$$|v_{\mathbf{k}}|^2 = \frac{1}{2}[1 - \xi(\mathbf{k})/E(\mathbf{k})],$$

$$|u_{\mathbf{k}}|^2 = \frac{1}{2}[1 + \xi(\mathbf{k})/E(\mathbf{k})],$$

$$u_{\mathbf{k}} v_{\mathbf{k}} = \Delta(\mathbf{k})/2E(\mathbf{k}), \tag{6}$$

with

$$E(\mathbf{k}) = \sqrt{\xi^2(\mathbf{k}) + |\Delta(\mathbf{k})|^2}.$$

The parameters $\xi(\mathbf{k})$ and $\Delta(\mathbf{k})$ are related to the particle-hole and particle-particle pairing amplitudes which are introduced below in Eqs. (7) and (8). $E(\mathbf{k})$ turns out to be the energy of a quasiparticle in the SC state.[4] We define

$$\Delta_\tau = \langle c_{i\uparrow}^\dagger c_{i+\tau\downarrow}^\dagger - c_{i\downarrow}^\dagger c_{i+\tau\uparrow}^\dagger \rangle, \tag{7}$$

$$\chi_\tau = \sum_\sigma \langle c_{i\sigma}^\dagger c_{i+\tau\sigma} \rangle, \tag{8}$$

with $\tau = \hat{x}, \hat{y}$, the NN unit vector. For the $d_{x^2-y^2}$ pairing symmetry, $\Delta_x = -\Delta_y = \Delta_0$, $\chi_x = \chi_y = \chi_0$, and $\xi(\mathbf{k})$, $\Delta(\mathbf{k})$ have the forms

$$\xi(\mathbf{k}) = g_t \varepsilon(\mathbf{k}) - \tilde{\mu} - \chi(\cos k_x + \cos k_y), \tag{9}$$

$$\Delta(\mathbf{k}) = \Delta(\cos k_x - \cos k_y), \tag{10}$$

where $\Delta = (3g_s J/4)\Delta_0$, $\chi = (3g_s J/4)\chi_0$, and $\tilde{\mu} = \mu + \partial \langle H' \rangle_0 / N \partial \delta$. The mean fields Δ_0 and χ_0 can be determined by solving these self-consistent Eqs. (5)–(10). The SC order parameter is defined as

$$\Delta_{\mathrm{SC}}(\mathbf{R}_{ij}) = \langle c_{i\uparrow}^\dagger c_{j\downarrow}^\dagger - c_{i\downarrow}^\dagger c_{j\uparrow}^\dagger \rangle,$$

which is related to the variational parameter Δ_0 in the Gutzwiller approximation[3,4]

$$\Delta_{\mathrm{SC}} = g_t \Delta_0. \tag{11}$$

C. Variational Monte Carlo method

In the VMC calculation, we first rewrite the wave function (2) in the Hilbert space with fixed number of N_e electrons doped with even number of n holes,

$$|\Psi_{\mathrm{RVB}}\rangle = P_G \left(\sum_{\mathbf{k}} \frac{v_{\mathbf{k}}}{u_{\mathbf{k}}} c_{\mathbf{k}\uparrow}^\dagger c_{-\mathbf{k}\downarrow}^\dagger \right)^{(N_e - n)/2} |0\rangle \tag{12}$$

with

$$\frac{v_{\mathbf{k}}}{u_{\mathbf{k}}} = \frac{\Delta_{\mathrm{MC}}(\mathbf{k})}{\epsilon_{\mathrm{MC}}(\mathbf{k}) + \sqrt{\epsilon_{\mathrm{MC}}(\mathbf{k})^2 + |\Delta_{\mathrm{MC}}(\mathbf{k})|^2}},$$

$$\epsilon_{\mathrm{MC}}(\mathbf{k}) = -2t(\cos k_x + \cos k_y) - 4t_v' \cos k_x \cos k_y - 2t_v''(\cos 2k_x + \cos 2k_y) - \mu_v,$$

$$\Delta_{\mathrm{MC}}(\mathbf{k}) = 2\Delta_v(\cos k_x - \cos k_y),$$

where Δ_v and μ_v are variational parameters, with Δ_v related to the d-wave SC order parameter and μ_v similar to the chemical potential. Note that we have used subscript "MC" to distinguish the parameters here from those adopted in the Sec. II B. We have also included two additional variational parameters t_v' and t_v'', which are usually not equal to the bare values t' and t'' because the constraint strongly renormalizes the hopping amplitudes. That is to say, the form of $\epsilon_{\mathrm{MC}}(\mathbf{k})$ in the variational wave function can be different from the dispersion function of the noninteracting electrons. These variational parameters determine the Fermi surface topology. Then, the quasiparticle excitations are created by adding holes into Eq. (12):

$$|\Psi_{\mathrm{exc}}(\mathbf{q})\rangle = P_G c_{\mathbf{q}\uparrow}^\dagger \left(\sum_{\mathbf{k}} \frac{v_{\mathbf{k}}}{u_{\mathbf{k}}} c_{\mathbf{k}\uparrow}^\dagger c_{-\mathbf{k}\downarrow}^\dagger \right)^{(N_e - n)/2 - 1} |0\rangle. \tag{13}$$

From Eq. (13) we calculate the energy dispersion for a given doping density by using VMC. The system used in this paper is of 12×12 sites with periodic boundary conditions.[30] We then fit the quasiparticle energy with the formula $a\sqrt{\varepsilon_{\mathbf{k}}^2 + \Delta_{\mathbf{k}}^2} - b$ to determine the renormalized parameters, with a and b the fitting parameters. Additionally, in order to eliminate the bias introduced in the trial wave function method, the power-Lanczos method which is a hybrid of the power and the variational Lanczos method is used to further improve the

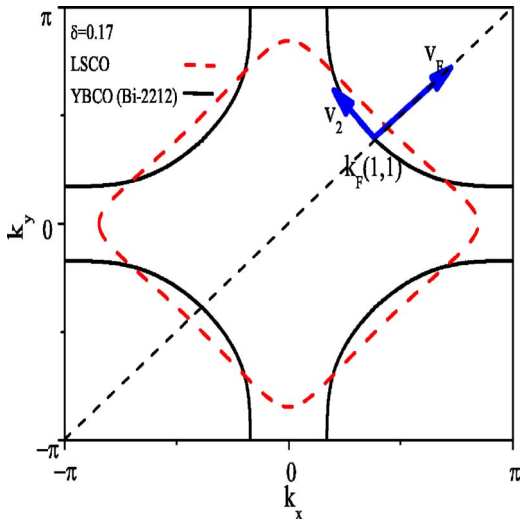

FIG. 1. (Color online) Illustration of the Fermi surface for LSCO (dashed square) and for YBCO (solid line), and the location of the gap nodes $k_F(\pm 1, \pm 1)$. The " Fermi velocity" v_F and the "gap velocity" v_2 are defined as the slopes of the quasiparticle energy along and perpendicular to the nodal direction. v_F and v_2 specify the Dirac cone for the nodal quasiparticle dispersion.

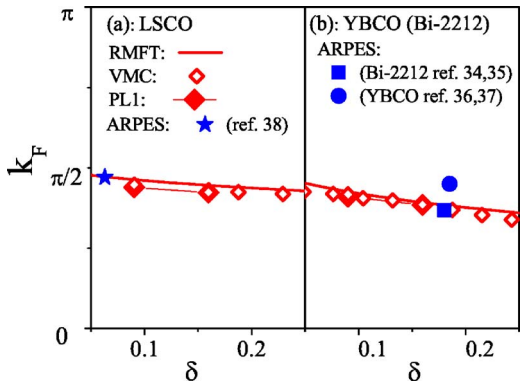

FIG. 2. (Color online) Comparison of the doping dependence of the Fermi wave vector k_F obtained from our theoretical calculation with those obtained by the ARPES for (a) LSCO and (b) YBCO (Bi-2212). (Refs. 34–38) Theoretical results are obtained using parameters listed in Table I for LSCO and YBCO (Bi-2212) with the in-plane lattice constant $a=3.8$ Å. RMFT: renormalized mean field theory; VMC: variational Monte Carlo; PL1: Power Lanczos to the first order. Note that the values from VMC and PL1 may be very close, and get overlapped with each other in some plots following.

trial function.[15,16] In the power method it can be easily shown that if a trial wave function $|\Psi\rangle$ is not orthogonal to the ground state, $(W-H)^m|\Psi\rangle$ is proportional to the ground state wave function as the power m approaches infinity. W is an appropriately chosen constant to make the ground-state energy the largest eigenvalue of the W-H matrix. In our calculation, the first order Lanczos method, i.e., $m=1$ is used and the improved trial wave function is $|\mathrm{PL1}\rangle=(1+C_1H)|\Psi\rangle$. C_1 is a new variational parameter. The results described below denoted as PL1 are calculated with the trial wave function $(1+C_1H)|\Psi\rangle$.

III. BASIC PARAMETERS

In this section, we discuss the parameters of nodal quasiparticles in the d-wave SC Cu oxides and make comparisons between the theory and experiments. It has been well established in experiments that the cuprate superconductivity has $d_{x^2-y^2}$-wave pairing.[31] There are four gap nodes in the $\mathbf{k}$ space, where the quasiparticle dispersion $E_{\mathbf{k}}=\sqrt{\xi_{\mathbf{k}}^2+\Delta_{\mathbf{k}}^2}$ approaches zero. The typical Fermi surface (FS) in HTSC is shown in Fig. 1, together with the "Fermi velocity" v_F and the "gap velocity" v_2 defined as the slopes of $E_{\mathbf{k}}$ along the directions perpendicular and tangential to the Fermi surface at the nodes $k_F(\pm 1, \pm 1)$. $\sqrt{2}k_F$ is the Fermi wave vector along the diagonal direction. Different from the conventional s-wave pairing symmetry, low energy quasiparticles in the vicinity of these nodes can be easily excited by thermal fluctuation, impurity scattering, or disorder effects. These low-energy nodal quasiparticles predominate physical properties of HTSC at low temperatures.

A. Fermi wave vector

From ARPES data, it is well known that a transition from a holelike Fermi surface centered at (π,π) to an electronlike Fermi surface centered at $(0,0)$ occurs slightly above the optimal doping in both LSCO and Bi-2212, meanwhile the Fermi wave vector k_F shifts just a little bit.[18,32,33] For Bi-2212, ARPES experiments[34] suggest that k_F is weakly doping dependent and $\sqrt{2}k_F \simeq 0.43$ Å^{-1}.[35] For optimally doped $YBCO_{6.95}$, $\sqrt{2}k_F \simeq 0.53$ Å^{-1},[36,37] and for underdoped $La_{2-x}Sr_xCu_2O_4$ ($x=0.063$), $\sqrt{2}k_F=0.55$ Å^{-1},[38] with the lattice constant $a=3.8$ Å. These experimental data are shown in Fig. 2, compared with our theoretical calculation where k_F is determined by $\xi(\mathbf{k})=0$ along the diagonal direction. For all the methods considered, we found that k_F decreases with increasing doping and k_F decreases more rapidly in YBCO (Bi-2212) than in LSCO. The values of k_F for the underdoped LSCO and optimally doped Bi-2212 and YBCO agree qualitatively with the experimental data.

B. Fermi velocity v_F

In the vicinity of the gap nodes, the quasiparticle dispersion can be expressed as

$$E(\mathbf{k}) = \sqrt{v_F^2 k_\parallel^2 + v_2^2 k_\perp^2},$$

where v_F (v_2) and $k_\parallel$ ($k_\perp$) are the components of the velocity and wave vector perpendicular (parallel) to the Fermi surface, respectively. The Fermi velocity extracted from the slope of the quasiparticle dispersion obtained by ARPES is found remarkably universal, independent of the doping concentration $v_F \approx 250 \sim 270$ km/s within an experimental error of $10-20$ %.[35,39]

In the RMFT, v_F and v_2 are given by the following equations:

$$v_F = \sqrt{2}|\sin k_F| \times \left| 2\left(g_t t + \frac{1}{2}\chi\right) - 4g_t|t'|\cos k_F + 8g_t t' \cos k_F \right|, \tag{14}$$

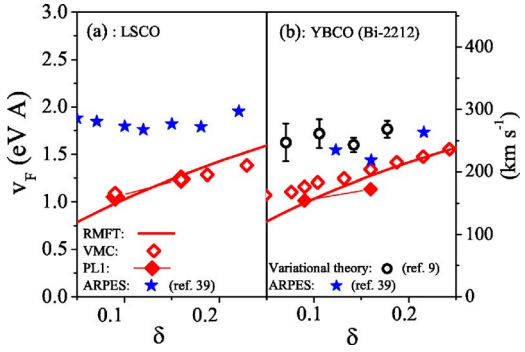

FIG. 3. (Color online) Fermi velocity v_F vs hole concentration δ. The results from variational theory in Ref. 9 were obtained with the correction of order of $O(J/t)$ included for the Hubbard model. (1 eV Å $\simeq$ 152 km/s).

$$v_2 = |\sqrt{2}\Delta \sin k_F|. \tag{15}$$

Shown in Fig. 3 is the value of v_F obtained from Eq. (14). v_F increases with doping. The VMC gives essentially the same result. In the optimally doped and overdoped regimes, this trend does not deviate greatly from the experimentally observed universality. However, the value of v_F appears underestimated in the RMFT for the extended t-J model compared with the experimental data and that obtained for the Hubbard model by including the correction of order of $O(J/t)$ reported previously by Paramekanti *et al.*[3,9]

C. "Gap velocity" v_2

The "gap velocity" v_2 is the slope of the SC energy gap along the Fermi surface at the gap node. Together with k_F and v_F, v_2 specifies the Dirac cone for the nodal quasiparticle dispersion. Among them v_2 plays a crucial role in determining the nodal physics of HTSC. This is because k_F and v_F are rather universal, depending weakly on the doping concentration. Furthermore, v_2 is much smaller than v_F, and many physical properties are related to v_2 in the form of the ratio v_F/v_2, therefore a small variation in v_2 may lead to a drastic change of v_F/v_2, hence of some physical quantities.

Experimentally, v_2 is difficult to be determined accurately. It depends strongly on the doping concentration and other material properties. A number of experiments may be used to extract v_2. These experiments include ARPES,[18,35] the temperature dependence of in-plane magnetic penetration depth $\lambda(T)$,[40] the electronic specific heat $C_{\rm el}$,[41–44] and the linear residual thermal conductivity $\kappa_0/T|_{T=0}$.[37,45–47] The linear residual thermal conductivity is robust against renormalization due to quasiparticle interactions and vertex corrections. In the SC state, $\kappa_0/T|_{T=0} \propto v_F/v_2 + v_2/v_F$ is universal and it does not depend on the impurity scattering rate.[48]

Figure 4 shows the doping dependence of v_2 and the ratio v_F/v_2. The calculation shows that v_2 drops quasilinearly with increasing doping. This behavior is consistent with the recent experiment of the magnetic field dependence of the specific heat on LSCO.[44] Our calculation gives $v_2 = 20 \sim 30$ km/s at optimal doping, which is larger than the experimentally reported value of $10 \sim 20$ km/s for YBCO (Bi-2212) obtained

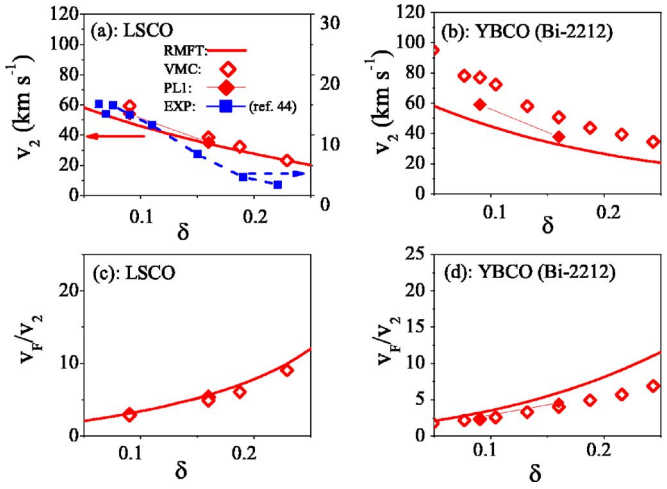

FIG. 4. (Color online) (a) and (b) " Gap velocity" v_2 vs hole concentration δ. For optimal doped YBCO (Bi-2212), $v_2 = 10 \sim 20$ km/s was reported by various kinds of experiments (Refs. 35, 37, and 46). The experimental data indicated in panel (a) is achieved by measuring the magnetic field dependence of the specific heat on LSCO at the zero temperature limit (Ref. 44). (c) and (d) the ratio v_F/v_2 vs hole concentration δ. The doping dependence of the ratio v_F/v_2 is similar to that observed in the thermal conductivity experiments (see Fig. 6).

from the thermal conductivity measurement[46,47] and ARPES,[35,37] and of 7 km/s for LSCO obtained from the measurements of magnetic field dependence of the specific heat at the zero temperature limit.[44] In the RMFT, $v_F/v_2 = 1$ at zero doping. As doping increases, v_F/v_2 increases rapidly. The doping dependence is qualitatively consistent with the data reported in the thermal conductivity measurements.[46,47]

In our theoretical calculation, despite of the great difference between the hopping integrals t' and t'' for YBCO (Bi-2212) and LSCO, the values of v_2 are only slightly different. This result is also in qualitative agreement with the thermal conductivity measurements. In the next section we will use our theoretical result of v_2 and v_F to extract some physical observables and compare them with experimental results.

IV. NODAL PHYSICS

In HTSC, d-wave pairing symmetry leads to a dome-like quasiparticle dispersion around the gap nodes. In the SC state, the gapless quasiparticle excitations in the vicinity of nodes dominate low-temperature physical properties. It is of fundamental importance to explore physical properties of these quasiparticle excitations.

In the clean limit, the density of states (DOS), $\rho(\omega)$, of low lying quasiparticles near the nodes is linear,

$$\rho(\omega) = \frac{2}{\pi} \frac{1}{v_F v_2} \omega. \tag{16}$$

The linear coefficient of $\rho(\omega)$ is inversely proportional to the nodal velocities v_F and v_2. This linearity in energy of $\rho(\omega)$ leads to many unconventional physical behaviors such as the quadratic electronic specific heat,[35,37,41,49] the linear residual

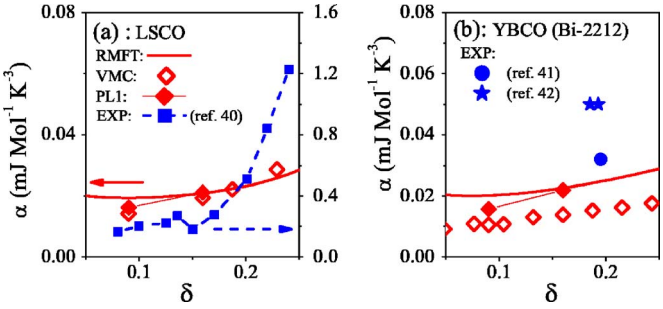

FIG. 5. (Color online) The quadratic coefficient of the electronic specific heat: $\alpha = C_{el}/T^2$ vs hole concentration δ.

thermal conductivity,[37,45,46,50] and the linear decreasing of superfluid density.[51,52] Experimental observations of these behaviors have provided some of the early evidences for unconventional $d_{x^2-y^2}$ pairing symmetry in HTSC. The nature of the interactions of nodal quasiparticles is not so clear in HSTC.[35,49] Some have used a renormalization factor to describe the effect of quasiparticle interactions on the electronic specific heat and on the in-plane magnetic penetration depth.[35,49] In this paper, we shall neglect quasiparticle interactions and set the renormalization factor to be unity.

A. Electronic specific heat

The linear low energy DOS $\rho(\omega)$ leads to a quadratic temperature dependence of the low-temperature electronic specific heat in the HTSC, given by

$$C_{el} = \gamma T = \alpha T^2, \alpha = \frac{21.6}{\pi}\frac{k_B^3}{\hbar^2}\frac{1}{v_F v_2}. \tag{17}$$

Figure 5 compares our theoretical results with the experiments for LSCO and YBCO.[40–42] The experimental result for LSCO shows a general tendency to increase as doping increases, and the rapid increase of α in the overdoped region might be due to the Fermi level crossing of the flat band at $(\pi,0)$, which yields one additional channel to thermally excite quasiparticles. In our theoretical results, the doping dependence of α is similar for LSCO and YBCO. The values of α are about $0.01 \sim 0.03$ mJ/mol K^3 which are comparable to the experimental value of YBCO,[41,42] but much smaller than the value of LSCO.[40]

B. Thermal conductivity

In the presence of a small amount of disorder or impurities, the nodal quasiparticles are delocalized and can carry both heat and charge. For dilute nonmagnetic impurities, there will be a residual normal fluid due to these delocalized and conductive quasiparticles. The most striking property of this conduction mechanism is the universal limit, i.e., the quasiparticle transport is independent of the scattering rate as $T \to 0$. With increasing the impurity concentration, the mean free path is reduced, but the normal fluid density increases.[48,53] In the SC state with a random distribution of impurities of an energy scale $E_{im} < k_B T_c$, the low-temperature thermal conductivity is linear,[48,53] and is given by

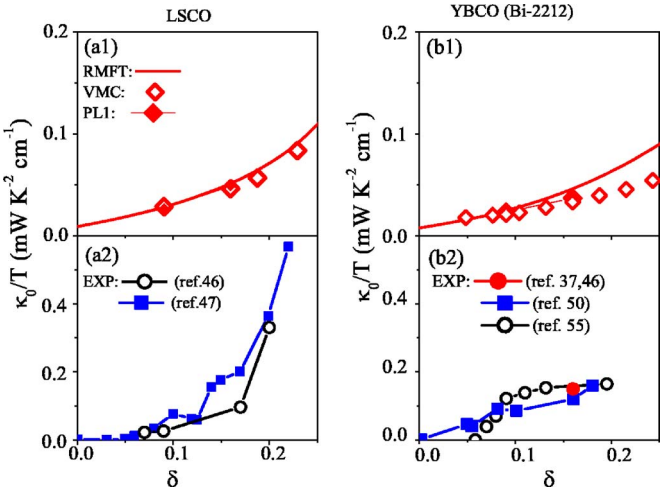

FIG. 6. (Color online) Linear residual thermal conductivity κ_0/T vs hole concentration δ.

$$\left|\frac{\kappa_0}{T}\right|_{T=0} = \frac{k_B^2}{3\hbar}\frac{n}{d}\left(\frac{v_F}{v_2}+\frac{v_2}{v_F}\right), \tag{18}$$

where d/n, the stacking distance between two nearest-neighboring CuO_2 planes, has the values of 6.6, 5.8, and 7.72 Å for LSCO, YBCO, and Bi-2212, respectively. This formula is obtained within the self-consistent T-matrix approximation, and it may break down if the impurity scattering gets too strong.[54] This universal behavior of the thermal conductivity provides a robust and direct measurement of v_F/v_2 in the SC state.

Figure 6 shows our theoretical results of $\kappa_0/T|_{T=0}$ compared with the experimental results for LSCO and YBCO (Bi-2212).[37,46,47,50,55] Experimentally, above a critical doping δ_{pc}, both LSCO and YBCO (Bi-2212) are thermal metals and $\kappa_0/T|_{T=0}$ increases steadily as δ in the underdoped regime and very rapidly in the overdoped regime. Such observation strongly supports the notion that there are well-defined nodal quasiparticles in the clean limit. The difference of the residual thermal conductivity between LSCO and YBCO (Bi-2212) is much smaller compared with the case for the electronic specific heat shown in Fig. 5. In the lightly underdoped regime $\delta < \delta_{pc}$, the low temperature behavior of κ_0/T remains unclear.[50,55] However, it is clear that $\kappa_0/T \to 0$ as $T \to 0$ in LSCO.[56,57] The thermal insulating behavior in LSCO is probably caused by the localization of quasiparticles due to disorder effects.

In our calculation, the SC state and the delocalized quasiparticles are assumed to prevail even in the heavily underdoped region. The theoretical results deviate from the experimental ones by a factor of 2–4. We attribute this discrepancy to the overestimated gap velocity v_2 in the theory.

C. In-plane magnetic penetration depth

The magnetic penetration depth $\lambda(T)$ is related to the superfluid density ρ_s by

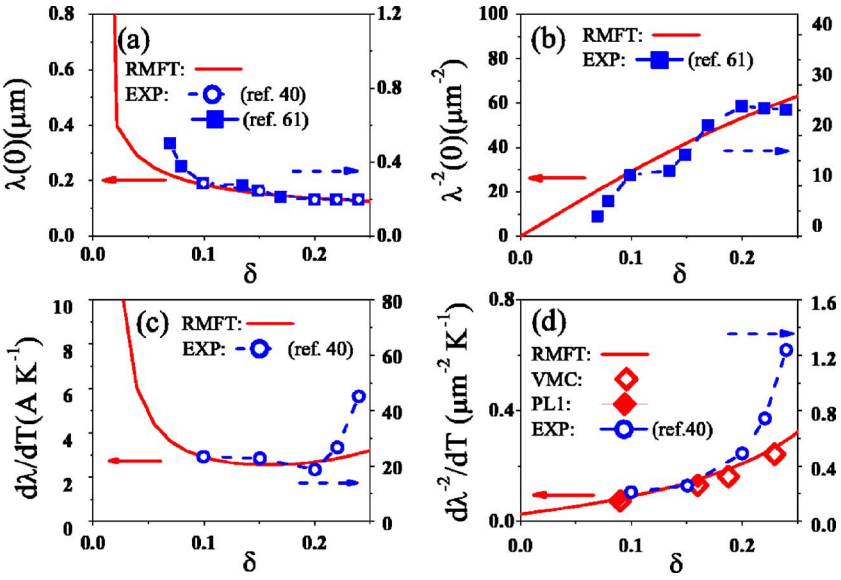

FIG. 7. (Color online) In-plane magnetic penetration depth in LSCO vs hole concentration δ.

$$\frac{\rho_s(T)}{m^*} = \frac{\rho_s(0)}{m^*} - \frac{\rho_n(T)}{m^*} = \frac{c^2}{4\pi e^2}\frac{1}{\lambda^2},$$

where m^* is the effective mass of the charge carriers and assumed to be doping independent, ρ_n is the normal fluid density.[51] At low temperatures, ρ_n is contributed from the thermally excited quasiparticles near nodes, and can be given by

$$\frac{\rho_n(T)}{m^*} = \left(\frac{2\ln 2}{\pi}\right)\frac{n v_F}{d v_2}\frac{k_B T}{\hbar^2}.$$

The linear temperature coefficient of $\rho_s(T)/m^*$ is proportional to v_F/v_2.

At low temperatures, the temperature dependence of $\lambda(T)$ is very weak, and $\lambda(0)$ is about several thousands angstroms.[40,52,58–61] The first and second derivatives of the penetration depth with respect to temperature can be expressed approximately as

$$\left|\frac{d\lambda(T)}{dT}\right|_{T\to 0} = \lambda^3(0) 4\ln 2 \frac{e^2}{c^2}\frac{k_B}{\hbar^2}\frac{n}{d}\frac{v_F}{v_2}, \tag{19}$$

$$\left|\frac{d}{dT}\lambda^{-2}\right|_{T\to 0} = -8\ln 2 \frac{e^2}{c^2}\frac{k_B}{\hbar^2}\frac{n}{d}\frac{v_F}{v_2}. \tag{20}$$

Panels (a) and (b) of Figs. 7–9 show the zero temperature in-plane magnetic penetration depth $\lambda(0)$ and $\lambda^{-2}(0)$. Experimentally, as δ increases, $\lambda(0)$ in LSCO monotonically decreases,[40,61] while $\lambda(0)$ in YBCO and in $Bi_2Sr_2Ca_{1-x}Y_xCu_2O_{8+\delta}$ increases with doping in the overdoped region.[62,63] The experimental results of $\lambda^{-2}(0)$ in LSCO and underdoped YBCO (Bi-2212) show a linear doping dependence, supporting the idea that the zero tempera-

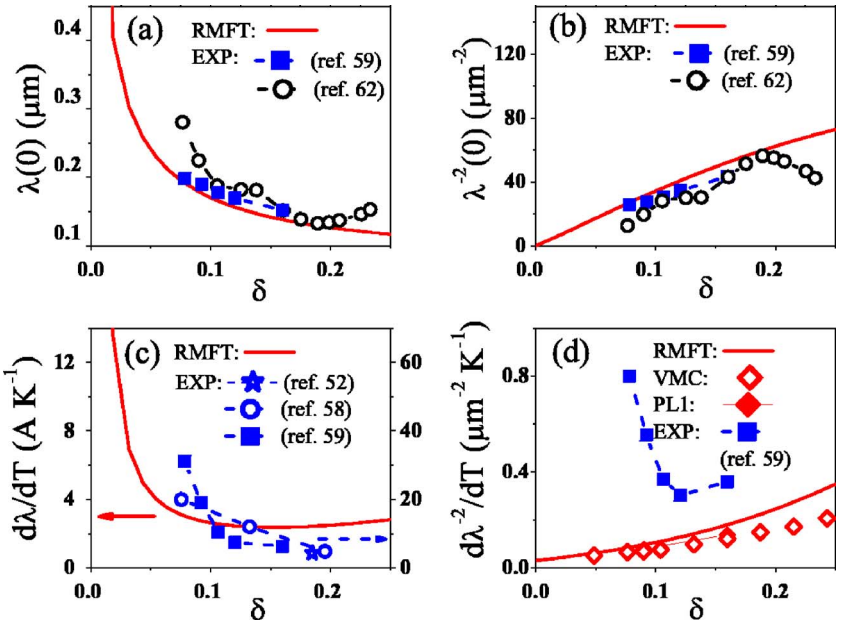

FIG. 8. (Color online) In-plane magnetic penetration depth in YBCO vs hole concentration δ.

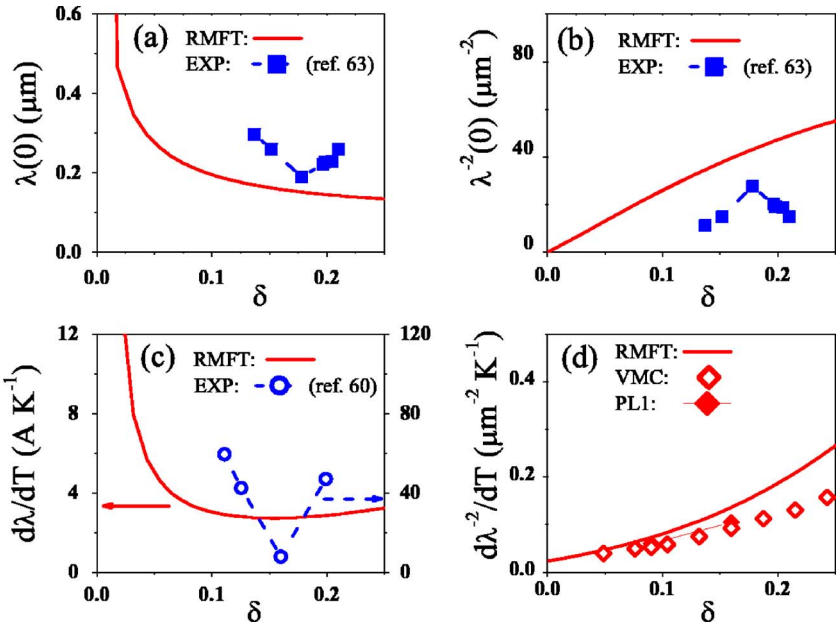

FIG. 9. (Color online) In-plane magnetic penetration depth in $Bi_2Sr_2Ca_{1-x}Y_xCu_2O_{8+\delta}$ vs hole concentration δ.

ture superfluid density $\rho_s(0)$ is proportional to the doping concentration in the underdoped region. In our RMFT, in the SC phase, $\lambda^{-2}(0)$ is nearly linear with the hole doping and $\lambda(0)$ diverges at zero doping within the approximation that all optical spectral weights are condensed to the zero energy in the *t-J* model. Our theoretical results of $\lambda(0)[\lambda^{-2}(0)]$ agree with the experimental data for LSCO and YBCO in the underdoped region. In $Bi_2Sr_2Ca_{1-x}Y_xCu_2O_{8+\delta}$, our theoretical results show a discrepancy with experiments.

Panels (c) and (d) of Figs. 7–9 show the derivatives of the penetration depth with respect to temperature, $d\lambda(T)/dT$ and $d\lambda^{-2}/dT$. In the underdoped or slightly overdoped region, $d\lambda(T)/dT$ decreases with increasing doping in all three compounds.[40,52,58–61] In the heavily overdoped region $d\lambda(T)/dT$ increases with doping in both LSCO and $Bi_2Sr_2Ca_{1-x}Y_xCu_2O_{8+\delta}$. In LSCO, $d\lambda^{-2}/dT$ increases steadily with doping.[40,61] In YBCO, an opposite tendency was observed in the underdoped region $\delta<0.10$.[59] The anomalous increase in the underdoped region was previously shown to qualitatively agree with the behavior resulted from the *d*-density wave state.[59,64,65] In our RMFT, similar doping dependence of $d\lambda(T)/dT$ is obtained. However, there is a great discrepancy on the absolute value between experiments and our theoretical results. We argue that some other mechanisms may be responsible for the large value of $d\lambda(T)/dT$ observed in experiments.[26]

V. OTHER PHYSICAL PROPERTIES

A. Drude weight

The Drude weight or the superfluid stiffness D is a measurement of superfluid condensation. In the linear-response theory, within the approximation that in the *t-J* model all optical spectral weights are condensed to zero energy, the Drude weight D can be given by[66]

$$D = \left(\frac{e^2}{4\pi\varepsilon_0\hbar^2}\right)^{-1}\left(\frac{n}{d}\right)^{-1}\frac{2}{\pi}\int_0^\infty d\omega\ \mathrm{Re}\ \sigma(\omega) = -\frac{\langle E_{\mathrm{kin}}\rangle}{2}. \tag{21}$$

D is related to the plasma frequency ω_p^* by $(\omega_p^*)^2/8 = \int_0^\infty d\omega\ \mathrm{Re}\ \sigma(\omega)$. In optical reflectivity measurements, the frequency dependent conductivities can be derived from the reflectivity spectra. By integrating the spectral weight below 1.25 eV, $(\omega_p^*)^2$ was found to vanish linearly with the decrease of doping concentration in the low doping regime, and for optimally doped YBCO $(\hbar\omega_p^*)^2 \simeq 4.5$ eV, i.e., $D \simeq 145$ meV, along the *a* axis (without the contribution from the CuO chain).[67]

Figure 10 shows the RMFT and VMC results for Drude weight. Our results agree with those obtained with a finite cut-off of the integration in Eq. (21) to get rid of the contri-

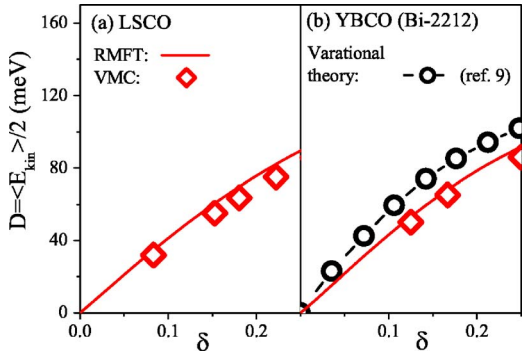

FIG. 10. (Color online) Drude weight D vs hole concentration δ. The results from the variational theory given in Ref. 9 are for the Hubbard model with a finite cutoff to get rid of the contribution due to transitions from the ground state to the "upper Hubbard band." In optical reflectivity measurements, the Drude weight is proportional to $(\omega_p^*)^2$, for optimally doped YBCO $(\hbar\omega_p^*)^2 \simeq 4.5$ eV, i.e., $D \simeq 145$ meV, along the *a* axis (Ref. 67).

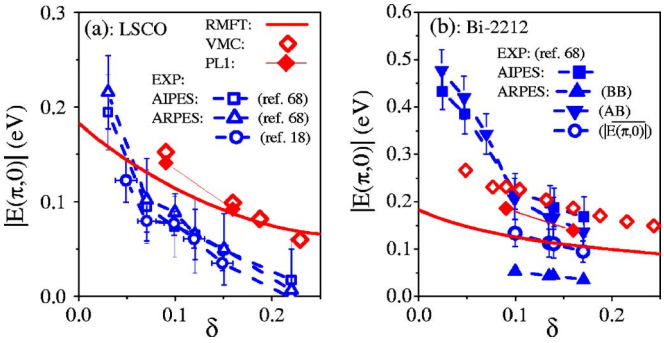

FIG. 11. (Color online) The quasiparticle energy $E(\pi,0)$ vs hole concentration δ.

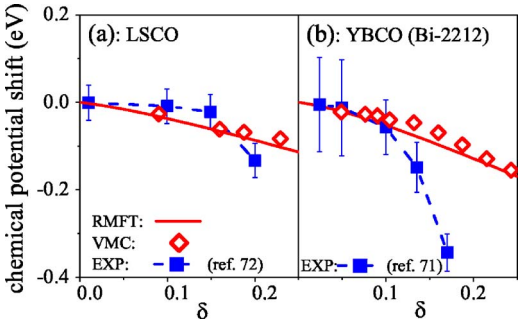

FIG. 12. (Color online) Chemical potential shift $\tilde{\mu}$ vs hole concentration δ. The experimental data were deduced from the shifts of photoemission and inverse-photoemission spectra of the core states of LSCO and Bi-2212 (Ref. 71 and 72).

butions due to transitions from the ground state to the "upper Hubbard band," those results include the correction of order of $O(J/t)$.[9] The Drude weight increases almost linearly in the underdoped regime. Around the optimal doping, our results of the Drude weight is about 60 meV, in agreement with the optical reflectivity experimental data given in Ref. 67.

B. The antinodal quasiparticle energy $E(\pi,0)$

Around the antinodal point $(\pi,0)$, the quasiparticle dispersion becomes flat. This flat band has been studied intensively by experiments.[18,32,68–70] In the RMFT study, the energy of quasiparticle excitations at $(\pi,0)$ is given by

$$E(\pi,0) = \sqrt{(-4g_t t' - 4g_t t'' - \tilde{\mu})^2 + 4\Delta^2}. \tag{22}$$

Figure 11 shows the doping dependence of $E(\pi,0)$ obtained in our calculation compared with the experimental results.[18,68] The experimental results obtained by angle-integrated photoemission spectroscopy and ARPES agree well with each other. In LSCO, the energy position of the flat band lies about 200–300 meV below the Fermi energy for lightly underdoped state, and is shifted up to the Fermi level quickly with increasing doping, finally crosses the Fermi level at optimal doping or slightly overdoping. In Bi-2212, two branches of flat bands (bonding band and antibonding band) were observed due to the bilayer splitting. They are determined by the low and high binding energies of the peak-dip-hump character. The average $\overline{E(\pi,0)}$ of the two bands is shown in Fig. 11(a).[68] The bonding band has the same doping dependence as that in LSCO. The antibonding band lies much higher than the bonding band.

In our calculation, without taking the bilayer coupling into consideration, our theoretical calculation of $E(\pi,0)$ in Bi-2212 should correspond to the average $\overline{E(\pi,0)}$. It approaches to the Fermi level with increasing doping, but does not get very close the Fermi level even in the overdoped regime. Similar doping dependence has been observed experimentally for $\overline{E(\pi,0)}$ in contrary to the approaching to the Fermi level in LSCO.[68] In VMC and PL1 simulation, the value of $E(\pi,0)$ is much closer to $\overline{E(\pi,0)}$ of Bi-2212 but is much larger than in LSCO.

C. Chemical potential shift

Figure 12 shows the electron chemical potential shift $\tilde{\mu}$, compared with experimental data for LSCO and Bi-2212.[71,72] In the RMFT, $\tilde{\mu}$ is given by

$$\tilde{\mu} = \mu + \frac{1}{N}\frac{\partial \langle H' \rangle_0}{\partial \delta}. \tag{23}$$

The experimental data were deduced from the shifts of photoemission and inverse-photoemission spectra of the core states of LSCO and Bi-2212. In LSCO the chemical potential shift $\tilde{\mu}$ was found to be pinned close to zero energy in underdoped regime.[71–73] In Bi-2212, the chemical potential shift is not pinned at zero energy and shows a more rigid-band-like behavior.[71]

In our calculations, the chemical potential shift agrees qualitatively with the experimental data. It is also consistent with the result obtained by the exact diagonalization of the t-t'-J model.[74] Furthermore, the shift is found to be larger in Bi-2212 than in LSCO in the entire hole doping range, in agreement with experiments.

D. Quasiparticle spectral weight

Figure 13 shows the nodal quasiparticle spectral weight Z. In ARPES experiments the quasiparticle spectral weight Z can be deduced from the spectral weight of the quasiparticle coherent peak at the gap nodes[33] or from the formula $Z = 1/(1+\lambda)$,[9] where the coupling constant λ can be extracted from the real part of self-energy $\mathrm{Re}[\Sigma(\mathbf{k},\omega)]$ of the spectral function.[75] In the RMFT analysis, the nodal quasiparticle spectral weight is equal to the renormalized factor of the hopping term g_t. Our theoretical results for the doping dependence of Z agree well with the experimental results. The nodal quasiparticle spectral weight grows almost linearly in

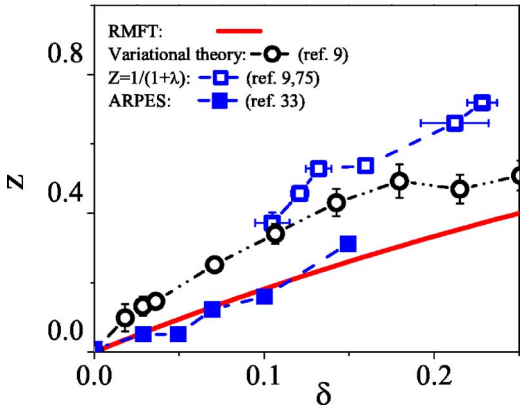

FIG. 13. (Color online) Nodal quasiparticle weight Z vs hole concentration δ. $Z=1/(1+\lambda)$ was estimated in Ref. 9, where λ is the coupling constant estimated from the spectra function in ARPES (Ref. 75). The results from VMC simulation is presented for a complementary comparison (Ref. 9).

the whole doping region as shown. The results from VMC are presented for a complementary comparison.[9]

E. Superconducting gap

Experimentally the maximal superconducting gap Δ_m can be measured by the thermal conductivity, ARPES, or other techniques. For example, from the thermal conductivity,[46] Δ_m can be determined by assuming $\Delta_m=\hbar k_F v_2/2$ with " universal" Fermi velocity v_F (Ref. 39) and "weakly" doping dependent k_F.[34] In ARPES, the midpoint shift of the leading edge of the quasiparticle spectral at $(\pi,0)$ is approximately equal to Δ_m. One can also determine Δ_m by fitting the gap dispersion on the Fermi surface with the formula $\Delta(\phi)=\Delta_m\cos 2\phi$, where ϕ is the Fermi surface angle.[72,76–79]

In Figs. 14(a) and 14(c), our theoretical results of $\Delta_m=\Delta(\cos k_x-\cos k_y)|_{\mathbf{k}=(\pi,0)}$ are shown and compared with the experimental data.[46,72,76,79] The doping dependence of Δ_m agrees with experiments, but the absolute values are about twice larger than the experimental ones in YBCO (Bi-2212).

Figures 14(b) and 14(d) compare the value of $\Delta_{SC}=g_t\Delta$ with the BCS gap $\Delta_{BCS}\simeq 2.14k_BT_c$ obtained by assuming $T_c=T_c^{\max}[1-82.6(\delta-0.16)^2]$ ($T_c^{\max}=95$ K for Bi-2212, 35 K for LSCO).[80] Δ_{SC} and Δ_{BCS} are roughly proportional to each other.

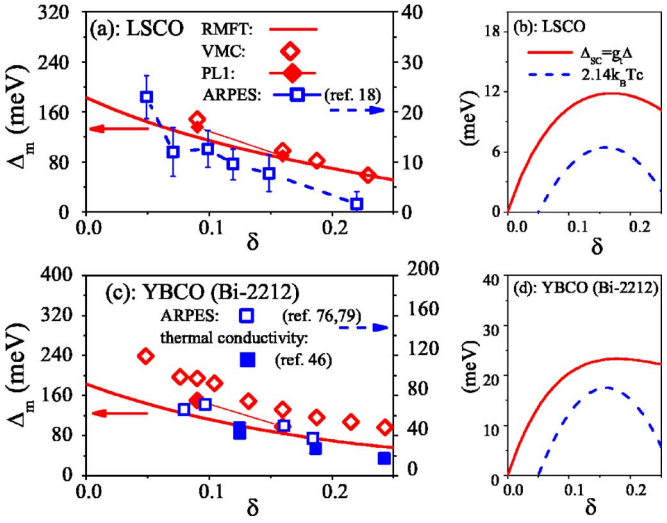

FIG. 14. (Color online) (a) and (c) The maximal superconducting gap Δ_m vs hole concentration δ. (b) and (d) Comparison of the superconducting order parameter $\Delta_{SC}=g_t\Delta$ in our RMFT calculation with the gap $\Delta_{BCS}=2.14k_BT_c$, where T_c is estimated from $T_c=T_c^{\max}[1-82.6(\delta-0.16)^2]$ ($T_c^{\max}=35$ K for LSCO and $T_c^{\max}=95$ K for Bi-2212) (Ref. 80).

VI. SUMMARY

In this paper we have made a systematic comparison between the plain vanilla RVB theory and a broad spectrum of experimental data of low-energy physical properties in cuprates. In our theoretical calculations with both RMFT and VMC, the only parameters are the spin coupling and the hopping integrals of electrons on the CuO_2 plane, which are known quite accurately. We have found a qualitatively good agreement between the theory and experiments on almost all the quantities we have studied, including the specific heat, the thermal conductivity, the in-plane magnetic penetration depth, the antinodal quasiparticle energy, the Drude weight, and the superconducting gap. The agreement on the doping dependences of these properties is remarkable except in the heavy overdoped regime. The major discrepancy is on the absolute values of some quantities, which may be attributed to the large value of v_2 estimated in the theory. The comparison would be quite satisfactory quantitatively if one had used a theoretical value of v_2 by 2–4 times smaller, which indicates a possibility of overestimate of the gap. (It is known that the gap estimated in the VMC calculation is overestimated by a factor of 2 or more.) This discrepancy could also be due to the simplification of the model Hamiltonian or the approximate wave function. More investigation will be needed to address these issues.

ACKNOWLEDGMENTS

This work was partially supported by the RGC grant in Hong Kong, and Grant No. NSC 94-2112-M-001-003, Taiwan.

[1] P. W. Anderson, Science **235**, 1196 (1987).
[2] F. C. Zhang and T. M. Rice, Phys. Rev. B **37**, R3759 (1988).
[3] P. W. Anderson, P. A. Lee, M. Randeria, T. M. Rice, N. Triveni, and F. C. Zhang, J. Phys.: Condens. Matter **16**, R755 (2004).
[4] F. C. Zhang, C. Gros, T. M. Rice, and H. Shiba, Supercond. Sci. Technol. **1**, 36 (1988).
[5] C. Gros, Phys. Rev. B **38**, R931 (1988); Ann. Phys. (N.Y.) **189**, 53 (1989); H. Yokoyama and H. Shiba, J. Phys. Soc. Jpn. **57**, 2482 (1988).
[6] T. K. Lee, C. T. Shih, Y. C. Chen, and H. Q. Lin, Phys. Rev. Lett. **89**, 279702 (2002); M. Ogata and A. Himeda, J. Phys. Soc. Jpn. **72**, 374 (2003).
[7] C. T. Shih, T. K. Lee, R. Eder, C.-Y. Mou, and Y. C. Chen, Phys. Rev. Lett. **92**, 227002 (2004); C. T. Shih, Y. C. Chen, C. P. Chou, and T. K. Lee, Phys. Rev. B **70**, 220502(R) (2004).
[8] G. Kotliar and J. Liu, Phys. Rev. B **38**, 5142 (1988); Y. Suzumura, Y. Hasegawa, and H. Fukuyama, J. Phys. Soc. Jpn. **57**, 2768 (1988); P. A. Lee, Phys. Rev. Lett. **63**, 680 (1989).
[9] A. Paramekanti, M. Randeria, and N. Trivedi, Phys. Rev. Lett. **87**, 217002 (2001); M. Randeria, A. Paramekanti, and N. Trivedi, Phys. Rev. B **69**, 144509 (2004); A. Paramekanti, M. Randeria, and Nandini Trivedi, *ibid.* **70**, 054504 (2004).
[10] P. W. Anderson and N. P. Ong, cond-mat/0405518 (unpublished); M. Randeria, R. Sensarma, N. Trivedi, and F. C. Zhang, Phys. Rev. Lett. **95**, 137001 (2005).
[11] F. C. Zhang, Phys. Rev. Lett. **90**, 207002 (2003); G. Baskaran, *ibid.* **90**, 197007 (2003); J. Y. Gan, Y. Chen, Z. B. Su, and F. C. Zhang, *ibid.* **94**, 067005 (2005); J. Liu, J. Schmalian, and N. Trivedi, *ibid.* **94**, 127003 (2005); R. Laughlin, cond-mat/0209269 (unpublished).
[12] B. Edegger, V. N. Muthukumar, C. Gros, and P. W. Anderson, cond-mat/0512646 (unpublished).
[13] Kai-Yu Yang, T. M. Rice, and Fu-Chun Zhang, Phys. Rev. B **73**, 174501 (2006).
[14] T. Yoshida, X. J. Zhou, K. Tanaka, W. L. Yang, Z. Hussain, Z.-X. Shen, A. Fujimori, S. Komiya, Y. Ando, H. Eisaki, T. Kakeshita, and S. Uchida, cond-mat/0510608 (unpublished).
[15] Y. C. Chen and T. K. Lee, Phys. Rev. B **51**, 6723 (1995).
[16] C. T. Shih, Y. C. Chen, and T. K. Lee, Phys. Rev. B **57**, 627 (1998).
[17] E. Pavarini, I. Dasgupta, T. Saha-Dasgupta, O. Jepsen, and O. K. Andersen, Phys. Rev. Lett. **87**, 047003 (2001).
[18] A. Ino, C. Kim, M. Nakamura, T. Yoshida, T. Mizokawa, A. Fujimori, Z.-X. Shen, T. Kakeshita, H. Eisaki, and S. Uchida, Phys. Rev. B **65**, 094504 (2002).
[19] A. Damascelli, Zhi-Xun Shen, and Z. Hussain, Rev. Mod. Phys. **75**, 473 (2003).
[20] K. B. Lyons, P. A. Fleury, L. F. Schneemeyer, and J. V. Waszczak, Phys. Rev. Lett. **60**, 732 (1988).
[21] J. M. Tranquada, G. Shirane, B. Keimer, S. Shamoto, and M. Sato, Phys. Rev. B **40**, 4503 (1989).
[22] R. Coldea, S. M. Hayden, G. Aeppli, T. G. Perring, C. D. Frost, T. E. Mason, S.-W. Cheong, and Z. Fisk, Phys. Rev. Lett. **86**, 5377 (2001).
[23] S. M. Hayden, G. Aeppli, P. Dai, H. A. Mook, T. G. Perring, S.-W. Cheong, Z. Fisk, F. Dogan, and T. E. Mason, Physica B **241-243**, 765 (1998).
[24] G. Blumberg, M. Kang, M. V. Klein, K. Kadowaki, and C. Kendziora, Science **278**, 1427 (1997).
[25] Shunji Sugai, Shin–ichi Shamoto, and Masatoshi Sato, Phys. Rev. B **38**, 6436 (1988).
[26] G. Blumberg, P. Abbamonte, M. V. Klein, W. C. Lee, D. M. Ginsberg, L. L. Miller, and A. Zibold, Phys. Rev. B **53**, R11930 (1996).
[27] M. C. Gutzwiller, Phys. Rev. Lett. **10**, 159 (1963).
[28] W. Brinkman and T. M. Rice, Phys. Rev. B **2**, 1324 (1970).
[29] D. Vollhardt, Rev. Mod. Phys. **56**, 99 (1984).
[30] The VMC results reported here are for H in Eq. (1) with an additional term of $(-1/4)n_i n_j$ in H_J. This additional term is a constant at half filling.
[31] C. C. Tsuei and J. R. Kirtley, Rev. Mod. Phys. **72**, 969 (2000).
[32] D. S. Dessau, Z.-X. Shen, D. M. King, D. S. Marshall, L. W. Lombardo, P. H. Dickinson, A. G. Loeser, J. DiCarlo, C.-H Park, A. Kapitulnik, and W. E. Spicer, Phys. Rev. Lett. **71**, 2781 (1993).
[33] T. Yoshida, X. J. Zhou, T. Sasagawa, W. L. Yang, P. V. Bogdanov, A. Lanzara, Z. Hussain, T. Mizokawa, A. Fujimori, H. Eisaki, Z.-X. Shen, T. Kakeshita, and S. Uchida, Phys. Rev. Lett. **91**, 027001 (2003).
[34] H. Ding, M. R. Norman, T. Yokoya, T. Takeuchi, M. Randeria, J. C. Campuzano, T. Takahashi, T. Mochiku, and K. Kadowaki, Phys. Rev. Lett. **78**, 2628 (1997).
[35] J. Mesot, M. R. Norman, H. Ding, M. Randeria, J. C. Campuzano, A. Paramekanti, H. M. Fretwell, A. Kaminski, T. Takeuchi, T. Yokoya, T. Sato, T. Takahashi, T. Mochiku, and K. Kadowaki, Phys. Rev. Lett. **83**, 840 (1999).
[36] M. C. Schabel, C.-H. Park, A. Matsuura, Z.-X. Shen, D. A. Bonn, R. Liang, and W. N. Hardy, Phys. Rev. B **57**, 6090 (1998).
[37] May Chiao, R. W. Hill, Christian Lupien, Louis Taillefer, P. Lambert, R. Gagnon, and P. Fournier, Phys. Rev. B **62**, 3554 (2000).
[38] X. J. Zhou, Junren Shi, T. Yoshida, T. Cuk, W. L. Yang, V. Brouet, J. Nakamura, N. Mannella, Seiki Komiya, Yoichi Ando, F. Zhou, W. X. Ti, J. W. Xiong, Z. X. Zhao, T. Sasagawa, T. Kakeshita, H. Eisaki, S. Uchida, A. Fujimori, Zhenyu Zhang, E. W. Plummer, R. B. Laughlin, Z. Hussain, and Z.-X. Shen, Phys. Rev. Lett. **95**, 117001 (2005).
[39] X. J. Zhou, T. Yoshida, A. Lanzara, P. V. Bogdanov, S. A. Kellar, K. M. Shen, W. L. Yang, F. Ronning, T. Sasagawa, T. Kakeshita, T. Noda, H. Eisaki, S. Uchida, C. T. Lin, F. Zhou, J. W. Xiong, W. X. Di, Z. X. Zhao, A. Fujimori, Z. Hussain, and Z. X. Shen, Nature (London) **423**, 398 (2003).
[40] C. Panagopoulos, B. D. Rainford, J. R. Cooper, W. Lo, J. L. Tallon, J. W. Loram, J. Betouras, Y. S. Wang, and C. W. Chu, Phys. Rev. B **60**, 14617 (1999).
[41] D. A. Wright, J. P. Emerson, B. F. Woodfield, J. E. Gordon, R. A. Fisher, and N. E. Phillips, Phys. Rev. Lett. **82**, 1550 (1999).
[42] Kathryn A. Moler, David L. Sisson, Jeffrey S. Urbach, Malcolm R. Beasley, Aharon Kapitulnik, D. J. Baar, R. Liang, and W. N. Hardy, Phys. Rev. B **55**, 3954 (1997).
[43] A. Junod, B. Revaz, Y. Wang, and A. Erb, Physica B **284-288**, 1043 (2000).
[44] Hai-Hu Wen, Lei Shan, Xiao-Gang Wen, Yue Wang, Hong Gao, Zhi-Yong Liu, Fang Zhou, Jiwu Xiong, and Wenxin Ti, Phys. Rev. B **72**, 134507 (2005).
[45] May Chiao, R. W. Hill, Christian Lupien, Bojana Popic, Robert Gagnon, and Louis Taillefer, Phys. Rev. Lett. **82**, 2943 (1999).
[46] M. Sutherland, D. G. Hawthorn, R. W. Hill, F. Ronning, S. Wakimoto, H. Zhang, C. Proust, Etienne Boaknin, C. Lupien, Louis Taillefer, Ruixing Liang, D. A. Bonn, W. N. Hardy, Robert Gagnon, N. E. Hussey, T. Kimura, M. Nohara, and H.

Takagi, Phys. Rev. B **67**, 174520 (2003).
[47] J. Takeya, Yoichi Ando, Seiki Komiya, and X. F. Sun, Phys. Rev. Lett. **88**, 077001 (2002).
[48] P. A. Lee, Phys. Rev. Lett. **71**, 1887 (1993).
[49] T. Xiang and C. Panagopoulos, Phys. Rev. B **61**, 6343 (2000).
[50] M. Sutherland, S. Y. Li, D. G. Hawthorn, R. W. Hill, F. Ronning, M. A. Tanatar, J. Paglione, H. Zhang, Louis Taillefer, J. DeBenedictis, Ruixing Liang, D. A. Bonn, and W. N. Hardy, Phys. Rev. Lett. **94**, 147004 (2005).
[51] P. A. Lee and Xiao-Gang Wen, Phys. Rev. Lett. **78**, 4111 (1997).
[52] W. N. Hardy, D. A. Bonn, D. C. Morgan, Ruixing Liang, and Kuan Zhang, Phys. Rev. Lett. **70**, 3999 (1993).
[53] A. C. Durst and P. A. Lee, Phys. Rev. B **62**, 1270 (2000).
[54] P. A. Lee, N. Ngaosa, and Xiao-Gang Wen, Rev. Mod. Phys. **78**, 17 (2006).
[55] X. F. Sun, Kouji Segawa, and Yoichi Ando, Phys. Rev. B **72**, 100502(R) (2005).
[56] N. E. Hussey, S. Nakamae, K. Behnia, H. Takagi, C. Urano, S. Adachi, and S. Tajima, Phys. Rev. Lett. **85**, 4140 (2000).
[57] D. G. Hawthorn, R. W. Hill, C. Proust, F. Ronning, Mike Sutherland, Etienne Boaknin, C. Lupien, M. A. Tanatar, Johnpierre Paglione, S. Wakimoto, H. Zhang, Louis Taillefer, T. Kimura, M. Nohara, H. Takagi, and N. E. Hussey, Phys. Rev. Lett. **90**, 197004 (2003).
[58] C. Panagopoulos, J. R. Cooper, and T. Xiang, Phys. Rev. B **57**, 13422 (1998).
[59] M. R. Trunin, Yu. A. Nefyodov, and A. F. Shevchun, Phys. Rev. Lett. **92**, 067006 (2004).
[60] G. Lamura, J. Le Cochec, A. Gauzzi, F. Licci, D. Di Castro, A. Bianconi, and J. Bok, Phys. Rev. B **67**, 144518 (2003).
[61] C. Panagopoulos, T. Xiang, W. Anukool, J. R. Cooper, Y. S. Wang, and C. W. Chu, Phys. Rev. B **67**, 220502(R) (2003).
[62] C. Bernhard, J. L. Tallon, Th. Blasius, A. Golnik, and Ch. Niedermayer, Phys. Rev. Lett. **86**, 1614 (2001).
[63] G. Villard, D. Pelloquin, and A. Maignan, Phys. Rev. B **58**, 15 231 (1998).
[64] Qiang-Hua Wang, Jung Hoon Han, and Dung-Hai Lee, Phys. Rev. Lett. **87**, 077004 (2001).
[65] Sumanta Tewari, Hae-Yong Kee, Chetan Nayak, and Sudip Chakravarty, Phys. Rev. B **64**, 224516 (2000).
[66] E. Dagotto, Rev. Mod. Phys. **66**, 763 (1994).
[67] S. L. Cooper, D. Reznik, A. Kotz, M. A. Karlow, R. Liu, M. V. Klein, W. C. Lee, J. Giapintzakis, D. M. Ginsberg, B. W. Veal, and A. P. Paulikas, Phys. Rev. B **47**, 8233 (1993).
[68] K. Tanaka, T. Yoshida, A. Fujimori, D. H. Lu, Z.-X. Shen, X.-J. Zhou, H. Eisaki, Z. Hussain, S. Uchida, Y. Aiura, K. Ono, T. Sugaya, T. Mizuno, and I. Terasaki, Phys. Rev. B **70**, 092503 (2004).
[69] D. S. Marshall, D. S. Dessau, A. G. Loeser, C-H. Park, A. Y. Matsuura, J. N. Eckstein, I. Bozovic, P. Fournier, A. Kapitulnik, W. E. Spicer, and Z.-X. Shen, Phys. Rev. Lett. **76**, 4841 (1996).
[70] K. Gofron, J. C. Campuzano, A. A. Abrikosov, M. Lindroos, A. Bansil, H. Ding, D. Koelling, and B. Dabrowski, Phys. Rev. Lett. **73**, 3302 (1994).
[71] N. Harima, A. Fujimori, T. Sugaya, and I. Terasaki, Phys. Rev. B **67**, 172501 (2003).
[72] A. Ino, T. Mizokawa, A. Fujimori, K. Tamasaku, H. Eisaki, S. Uchida, T. Kimura, T. Sasagawa, and K. Kishio, Phys. Rev. Lett. **79**, 2101 (1997).
[73] K. Yamada, C. H. Lee, K. Kurahashi, J. Wada, S. Wakimoto, S. Ueki, H. Kimura, Y. Endoh, S. Hosoya, G. Shirane, R. J. Birgeneau, M. Greven, M. A. Kastner, and Y. J. Kim, Phys. Rev. B **57**, 6165 (1998).
[74] T. Tohyama and S. Maekawa, Phys. Rev. B **67**, 092509 (2003).
[75] P. D. Johnson, T. Valla, A. V. Fedorov, Z. Yusof, B. O. Wells, Q. Li, A. R. Moodenbaugh, G. D. Gu, N. Koshizuka, C. Kendziora, Sha Jian, and D. G. Hinks, Phys. Rev. Lett. **87**, 177007 (2001).
[76] M. R. Norman, H. Ding, M. Randeria, J. C. Campuzano, T. Yokoya, T. Takeuchi, T. Takahashi, T. Mochiku, K. Kadowaki, P. Guptasarma, and D. G. Hinks, Nature (London) **392**, 157 (1998).
[77] H. Ding, M. R. Norman, J. C. Campuzano, M. Randeria, A. F. Bellman, T. Yokoya, T. Takahashi, T. Mochiku, and K. Kadowaki, Phys. Rev. B **54**, R9678 (1996).
[78] J. C. Campuzano, H. Ding, M. R. Norman, H. M. Fretwell, M. Randeria, A. Kaminski, J. Mesot, T. Takeuchi, T. Sato, T. Yokoya, T. Takahashi, T. Mochiku, K. Kadowaki, P. Guptasarma, D. G. Hinks, Z. Konstantinovic, Z. Z. Li, and H. Raffy, Phys. Rev. Lett. **83**, 3709 (1999).
[79] P. J. White, Z.-X. Shen, C. Kim, J. M. Harris, A. G. Loeser, P. Fournier, and A. Kapitulnik, Phys. Rev. B **54**, R15669 (1996).
[80] M. R. Presland, J. L. Tallon, R. G. Buckley, R. S. Liu, and N. E. Flower, Physica C **176**, 95 (1991).